REVIEW ARTICLE

Bedload transport through emergent vegetation: current status and its future prospect

Antonino D'Ippolito[1] · Francesco Calomino[1] · Subhasish Dey[2] · Roberto Gaudio[1] · Nadia Penna[1]

Abstract

Vegetation present in the water streams, on the banks and in the floodplain areas largely affects the river hydraulics. Indeed, river vegetation significantly influences hydrodynamics, sediment transport, bedforms, and pollutant transport. Environmental management of rivers requires an understanding of the various processes and predictive capabilities of models. In the past, many studies were conducted, especially in laboratory settings, in order to quantify flow resistance due to vegetation. It is only recently that the effects of vegetation on sediment transport came to the attention of researchers. In particular, both suspended and bedload transport were considered. This paper reviews recent works conducted on the effect of vegetation on incipient sediment motion and bedload transport. With regard to the incipient sediment motion, methods based on critical velocity, turbulence, vegetation drag, and velocity in the bed roughness boundary layer have been discussed. For bedload transport, methods based on bed shear stress, turbulent kinetic energy, a revisiting of classical formulas for estimating bedload transport in non-vegetated channels, and estimation from erosion around a single vegetation stem are analyzed. Finally, indications on further research and new development are provided.

Article Highlights

- Incipient sediment motion in vegetated channels is different from that in bare channels
- New models for the estimation of sediment transport in vegetated channels consider turbulence effects
- The presence of vegetation in rivers contributes in promoting the stability of the streambed

---

✉ Nadia Penna
  nadia.penna@unical.it

[1] Dipartimento di Ingegneria Civile, Università della Calabria, 87036 Rende, CS, Italy

[2] Department of Civil Engineering, Indian Institute of Technology Kharagpur, Kharagpur 721302, West Bengal, India

1 Introduction

River vegetation, independently from the location (in the channel, along the banks or on the floodplain), has a profound influence on the functioning of the fluvial system and gives recreational opportunities and aesthetic beauty [1]. River vegetation influences flow magnitude, hydraulic roughness, vertical velocity profile, turbulence regime, sediment transport, bank stability, stream temperature, and nutrient transport. There is a mutual feedback relationship among these different aspects. Environmental management of rivers requires an understanding of the various processes and predictive capabilities of models [2]. This is even more important considering that efforts are currently taken up worldwide for river restoration, renaturalization and rehabilitation of watersheds and watercourses [3–7].

The analysis of the interaction between fluid flow and vegetation is a fairly complex issue, owing to both the different physical mechanisms playing a role in the phenomenon, the biomechanical properties (size, shape, stiffness) characterizing the different types of vegetation, and their density and distribution. Under a strictly hydraulic viewpoint, vegetation clutters up part of the rivers cross-section, increases the roughness, and reduces the velocity; all these aspects result in increased water levels and, consequently, growing risk of floods. On the scale of the hydrographic network, the general velocity reduction influences the travel time of water particles, making the peak flow control easier [8, 9].

Several literature studies were carried out in the past with the aims of experimentally quantifying the flow resistance induced by vegetation [10–12], determining the effects due to the shear stress on the bed and the banks [13, 14], assessing the velocity distribution and the turbulence characteristics of the flow [15–22], evaluating the effects of finite-sized vegetation patches [23–31], analyzing the interaction between jets and vegetation [32, 33], studying transport and dispersion processes due to turbulence [34, 35], investigating the flow resistance in the case of one-line emergent vegetation [36, 37], and exploring the main hydrodynamic features of real vegetated water bodies [38, 39]. Many numerical studies were also conducted to better comprehend the interaction between flow and vegetation in terms of flow fields [40–42]. Recently, remote sensing were used to detect the presence of vegetation along watercourses and its characteristics [43–49].

Under a general viewpoint, and in virtue of their different behavior, in the literature one usually distinguishes between flow cases with rigid and flexible vegetation and, according to the water depth, as emergent, submerged and floating vegetation.

In the case of sediment erosion or deposition, the flow in open channels with submerged vegetation presents very different characteristics from those with emergent vegetation. In fact, while in the case of emergent vegetation the sediment deposition does not affect the distribution of velocity and turbulence, since the water depth remains constant, in the case of submerged vegetation, the height of the vegetation is reduced and both velocity and turbulence are modified. In any case, the distribution of velocity and turbulence is very different in the presence of emergent or submerged vegetation [50–53]. A schematic representation of the velocity distribution in the two cases is shown in Figs. 1a and 1b, respectively.

Sediment transport mainly includes bedload transport and suspended-load transport. In this paper, we limited the study to the former, i.e., grains moving in the vicinity of the bed, more or less confined within a relatively thin layer, rolling or sliding or jumping, so that the
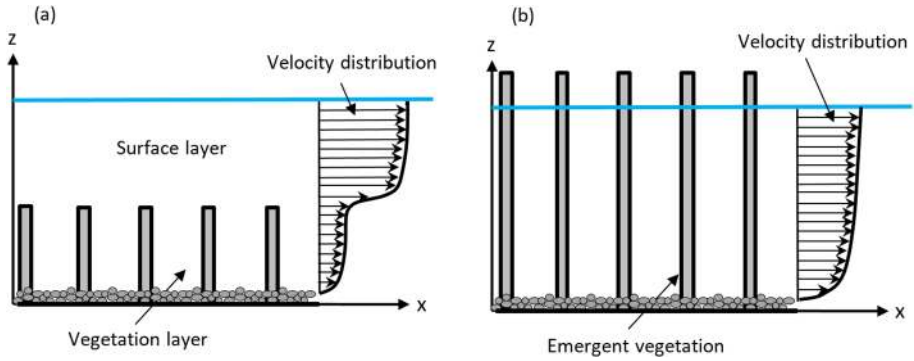
Fig. 1 Schematic representation of the velocity distribution along the water depth in the case of **a** submerged and **b** emergent vegetation

sediment remains in contact with the bed a large percentage of time. Experimental studies on bedload transport in vegetated flows were usually conducted in flumes with emergent rigid vegetation, which were simulated by using circular cylinders with uniform size and homogeneous distribution. The use of well-defined elements, such as circular cylinders, allows their accurate geometrical description, that is inherently variable in nature. A critical and detailed analysis of the use of circular cylinders to represent vegetation was carried out by Vargas-Luna et al. [54]. In the tests analyzed in the following sections, the used arrangements of the cylindrical elements representing the vegetation were linear, staggered and random; these are shown in Figs. 2a, 2b and 2c, respectively.

The purpose of this review is to feature research progress related to the role of vegetation on bedload transport. In Sect. 2 we analyze the studies for the incipient sediment motion in vegetated open-channel flows. Section 3 describes the different models for
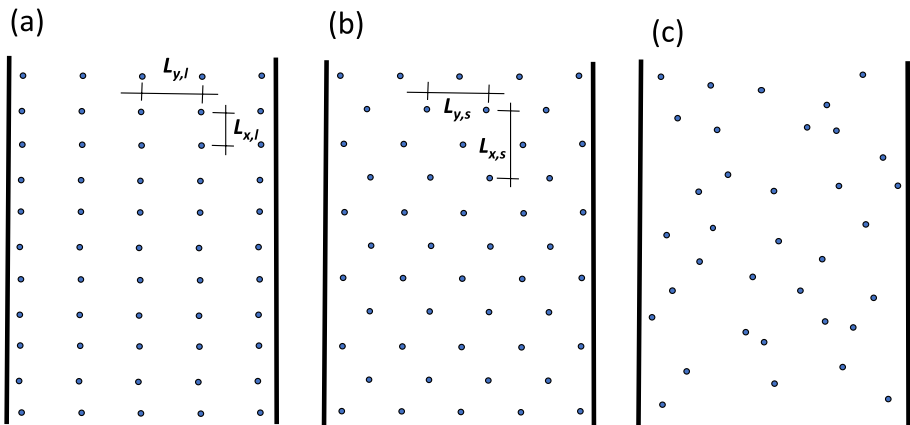
Fig. 2 Plan view of, **a** linear, **b** staggered and **c** random vegetation pattern. Here, $L_{x,l}$ and $L_{y,l}$ are the distances between the stems in the streamwise and spanwise directions, considering the linear pattern; whereas, $L_{x,s}$ and $L_{y,s}$ are the same distances in the staggered vegetation pattern

bedload transport, while in Sect. 4 we discuss the effect of vegetation on bed morphology. Finally, in Sect. 5 we provide some suggestions for the future research.

2 Incipient sediment motion in the presence of emergent rigid vegetation

This section presents classical methods for quantifying incipient sediment motion conditions along with more recently proposed methods. The formers are based on critical shear stress and critical flow velocity, while the most recent ones involve turbulence, vegetation drag and velocity in bed roughness boundary layer.

It should be noted that there is no standard method for measuring the critical velocity of incipient sediment motion in the case of vegetated channels.

With reference to the emergent rigid vegetation schematized by means of cylindrical elements of different materials, the experimental data usually used in the calibration and validation of the models refer to the data of Hongwu et al. [55] and Yang and Nepf [56]. Hongwu et al. [55] calculated the critical velocity as the velocity for which there was net sediment transport downstream of the vegetated zone. In fact, as will be better illustrated below, in some cases there may be local sediment movement near the cylindrical elements, but this does not result in sediment transport. In the case of the data from Yang and Nepf [56], the critical velocity was estimated identifying video noise levels, which were induced by moving particle tracers.

Depending on the characteristics of the velocity field and turbulence near the bed, a sediment particle can start moving in three different ways: lifting, sliding or rolling. A typical sediment particle is subject to the following forces (Fig. 3): submerged weight force (W), lift force (F_L), and drag force (F_D).

The critical conditions of incipient sediment motion in the case of lifting derives from the balance of forces along the vertical direction ($F_L = W$), in the case of sliding from the
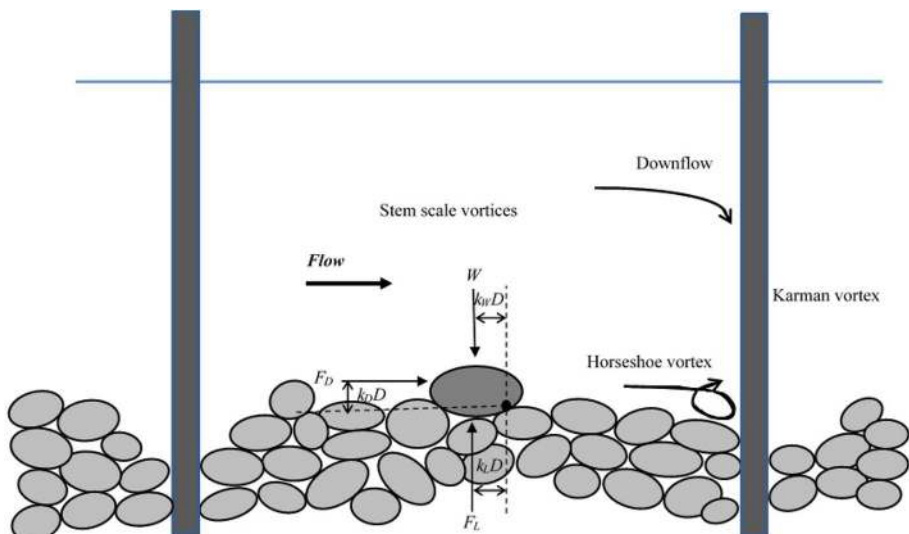

Fig. 3 Forces exerting on a bed particle

balance in the flow direction [$F_D = f(W - F_L)$] (where f is the friction coefficient of the sediment bed), and in the case of rolling from the balance of moments of forces with respect to the pivot point of rotation ($k_D F_D + k_L F_L = k_W W$, where k_D, k_L and k_W are the ratios of moment arm to particle diameter, which are related to the drag force, lift force, and submerged weight, respectively). Depending on how different authors expressed the above forces, several expressions of incipient sediment motion were provided.

Hongwu et al. [55] analyzed the incipient sediment motion in open channels in the presence of emergent rigid vegetation by carrying out experiments with rigid cylinders of circular cross-sectional shape arranged in a regular pattern. They used the flow velocity as a criterion for the incipient sediment motion, whereby there was continuous sediment transport outside the vegetated area, when the bedforms were in equilibrium. Based on experimental observations, three different regimes were identified. For small velocities, there was no sediment movement in the river bed. Above a certain velocity threshold, the sediments around some cylinders moved, resulting in a scour hole that became progressively deeper and wider until the equilibrium was reached; however, the authors reported that this did not result in sediment transport. With a further increase in flow velocity, considerable sediment transport occurred out of the scour holes and outside the vegetated area. By imposing equilibrium between the drag force and the difference between the weight and the lift force multiplied by the friction coefficient, and also considering the flow depth, h, the diameter of the stems, D, the mean sediment size, d, the vegetation density λ [with reference to the symbols shown in Fig. 2 in the case of linear arrangement $\lambda = (\pi D^2)/(4 L_{x,l} L_{y,l})$, while in the case of staggered arrangement $\lambda = (\pi D^2)/(2 L_{x,s} L_{y,s})$], Hongwu et al. [55] proposed the following equation:

$$V_c = 1.14 \sqrt{\frac{\gamma_s - \gamma}{\gamma} g d} \left(\frac{h}{d}\right)^{1/6} \times 0.316 \left(\frac{D \sqrt{\frac{\pi/4 - \lambda}{\lambda}}}{\sqrt{hd}}\right)^{0.319}, \tag{1}$$

where V_c is the critical spatially averaged velocity for incipient motion in a vegetated channel, γ and γ_s are the specific weight of water and sediment, respectively, and g is the acceleration of gravity. Equation (1) can be expressed in dimensionless terms as:

$$\frac{V_c}{V_{c0}} = 0.316 \left(\frac{D \sqrt{\frac{\pi/4 - \lambda}{\lambda}}}{\sqrt{hd}}\right)^{0.319}, \tag{2}$$

where:

$$V_{c0} = 1.14 \sqrt{\frac{\gamma_s - \gamma}{\gamma} g d} \left(\frac{h}{d}\right)^{1/6}, \tag{3}$$

is the flow velocity in the case of incipient sediment motion in the absence of vegetation. The relationship well fits the experimental data collected by the authors. In some cases, the velocity at which sediment transport begins in the presence of vegetation is lower than the one in the absence of vegetation. This is attributed to the secondary flows determined by the vegetation, which include downward flow in front of the rigid cylinders, a horseshoe vortex at the base of the cylinders, and wake eddies downstream of the cylinders.

More recent studies support the role of turbulence in the initiation of sediment motion. In fact, the passage of turbulent eddies and the associated fluctuations in the near-bed pressure generate sufficient instantaneous lift and drag forces to destabilize the grains. The magnitude of turbulence-induced fluctuating pressure scales with the magnitude of velocity fluctuation squared. Since the turbulent kinetic energy (TKE) is defined as $k_t = 0.5(\overline{u'^2} + \overline{v'^2} + \overline{w'^2})$, with the overbar indicating the time-average, and u', v', and w' denoting the turbulent velocity fluctuations in the streamwise, spanwise, and vertical directions, respectively, the pressure scales with TKE. Thus, the lift force is proportional to k_t [56]. In a bare channel, the TKE and the bed shear stress are linearly related, so that it is indifferent to refer to the one or the other. Also, the bed shear stress is proportional to the time-mean, depth-averaged velocity squared with a coefficient dependent on the bed roughness. In a vegetated channel, both the bed-generated, k_{tb}, and the vegetation-generated, k_{tv}, turbulence contribute to the near-bed TKE k_t, which is considered as the sum of the two, neglecting any mutual influence.

Yang et al. [57] in the case of sparse emergent vegetation, defined by $D/s_n < 0.56$ with s_n denoting the average surface-to-surface distance between the nearest stem neighbor, proposed to estimate the TKE as follows:

$$k_t = C_b V^2 + \delta_{k_t} \left[C_D \frac{\phi}{(1-\phi)\pi/2} \right]^{2/3} V^2, \tag{4}$$

where C_b is a coefficient dependent on the bed roughness, V is the bulk velocity (in the case of rectangular cross-section $V = Q/(Bh(1-\lambda)$, Q is the discharge, B is the width), C_D is the stem drag coefficient, ϕ is the solid volume fraction within the canopy (when the vegetation is represented by cylinders it is equal to $(\pi D^2/4)/\Delta S^2$, with ΔS being the average spacing between the cylinders; the solid volume fraction in the case of linear or staggered distribution with constant diameter of the cylinders representing the vegetation is equal to the vegetation density λ) and δ_{kt} is a coefficient equal to 1.2. In Eq. (4) the first term of the second member is the turbulence generated by the bed and the second one is the turbulence generated by the vegetation. In the experimental tests, since $D/s_n < 0.25$, i.e. $\phi \leq 5\%$, Eq. (4) was approximated by the authors as:

$$k_t = C_b V^2 + 0.9 C_D^{2/3} \phi^{2/3} V^2. \tag{5}$$

If k_t is the value of the TKE for which sediment transport initiates, the corresponding critical velocity can be determined from Eq. (5). Considering a channel without vegetation, having a bed with a particle size similar to that of the vegetated channel, Yang et al. [57] obtained that:

$$C_b V_c^2 + 0.9 C_D^{2/3} \phi^{2/3} V_c^2 = C_b V_{c0}^2, \tag{6}$$

where V_{c0} is the critical average velocity in the channel without vegetation, i.e. $V_c = V_{c0}$ when $\phi = 0$. From Eq. (6) it is possible to obtain:

$$\frac{V_c}{V_{c0}} = \frac{1}{\sqrt{1 + C\phi^{2/3}}}, \tag{7}$$

where $C = 0.9 C_D^{2/3}/C_b$.

Equation (1) was derived by Hongwu et al. [55] from the velocity distribution of the mean flow, although without determining its structure analytically; instead, Eq. (7) was derived by Yang et al. [57] assuming that the TKE plays a key role in determining the incipient sediment motion. Cheng et al. [58] asserted that, although both the mean flow and the TKE play different roles in the process of incipient sediment motion in a vegetated channel, they are still interconnected and should be considered in an integrated manner. From the equation of the balance of forces acting on a single particle, Cheng et al. [58] calculated a spatial and temporal average, and performed a scaling analysis based on the phenomenological theory of turbulence, arriving at the following equation in the case of sparse vegetation:

$$\frac{V_c}{\sqrt{\frac{\gamma_s - \gamma}{\gamma} g d}} = \sqrt{\frac{\alpha}{1 + \beta \lambda^{2/3}}}, \tag{8}$$

where α and β are two constants equal to 5 and 28, respectively, on the basis of the experimental data of Yang et al. [57] and Hongwu et al. [55]. The experimental data are well fitted by Eq. (8) with an average and maximum value of the prediction errors of 5.8% and 16.2%, respectively.

It is evident from the above that the incipient sediment motion in vegetated channels depends on the distribution of velocity and turbulence. Both the mean flow and the TKE in the case of vegetated channels are related to the drag force due to vegetation, thus, it plays a vital role in the incipient sediment motion in vegetated channels.

Wang et al. [59] considered the forces acting on a single particle and introduced into them the parameters reflecting the resistance of the vegetation ($C_D ah$), where a is the frontal area of the vegetation per unit volume, arriving at the following equation:

$$\frac{V_c}{V_{c0}} = 1 + k_1 (C_D ah)^{\beta_1}, \tag{9}$$

where k_1 and β_1 are two dimensionless coefficients. For the critical velocity of incipient sediment motion in the case of a bare bed, Wang et al. [59] used the equation proposed by Zhang et al. [60]:

$$V_{c0} = 1.34 \sqrt{\frac{\gamma_s - \gamma}{\gamma} g d} \left(\frac{h}{d}\right)^{1/7}. \tag{10}$$

Substituting Eq. (10) into Eq. (9) it gives:

$$\frac{V_c}{\sqrt{\frac{\gamma_s - \gamma}{\gamma} g d}} = 1.34 \left(\frac{h}{d}\right)^{1/7} \left[1 + k_1 (C_D ah)^{\beta_1}\right]. \tag{11}$$

The authors determined the parameters k_1 and β_1 from the data of Hongwu et al. [55], obtaining $k_1 = -0.55$ and $\beta_1 = 0.24$. For the estimation of C_D, they referred to the method proposed by Wang et al. [61]. The proposed formula was then validated by comparing the experimental and measured data of Yang et al. [57]. Specifically, for $C_D = 1.0$ they obtained a coefficient of determination $R^2 = 0.88$.

Recently Wang et al. [62] proposed a new formula for the critical flow velocity to predict incipient sediment motion. They referred to the velocity distribution in the bed roughness boundary layer introduced by Jeon et al. [63]. Based on experimental

observations, it can be assumed that, in the case of vegetated open-channel flows, the velocity is constant along the vertical excluding a small layer, namely the bed rough-ness boundary layer thickness, where there is a shear flow. Jeon et al. [63] showed that the velocity distribution in this layer is logarithmic. Starting from a general expression of the critical velocity near the bed, in the case of a hydrodynamically rough bed, and considering a logarithmic velocity distribution, Wang et al. [62] proposed the following equation:

$$V_c = c_2 ln\left(c_3 \frac{h}{d} \frac{0.008}{0.008 + \lambda h}\right)\sqrt{\Delta g d}.$$

(12)

where $\Delta = (\rho_s - \rho)/\rho$ is the submerged specific relative density of the sediment material, ρ_s and ρ are the sediment and water density, respectively. Based on the data of Hongwu et al. [55], Wang et al. [62] assumed for the constants c_2 and c_3 (functions of the ratio between the equivalent roughness of sediments and the thickness of the viscous sublayer) the values 0.29 and 34.87, respectively. The model was validated with the experimental data of Yang et al. [57] presenting a correlation coefficient between measured and calcu-lated critical velocities equal to $R^2 = 0.8$. The thickness of the bed roughness boundary layer is a function of the density of the vegetation and the formula proposed by Jeon et al. [63] for its determination was verified by Wang et al. [62] using other literature data. When sediment particles protrude outside the bed roughness boundary layer there is a redistribu-tion of velocity, the prediction of incipient sediment motion is affected, and its estimates are less accurate. The proposed model was also extended to the case of submerged vegeta-tion. The formula proposed by Wang et al. [62] is valid in the case of hydraulically rough beds with uniform non-cohesive fine grains. The coefficients in the formula were derived from experimental test data in which vegetation was simulated using rigid cylinders.

3 Bedload transport

Models for the estimation of bedload transport rate in vegetated channels were initially based on time-averaged bed shear stress [2, 4]. Subsequent studies showed how this was correlated with the TKE [57, 64]. More recently, classical formulas for estimating bedload transport rate in channels without vegetation were revisited and extended to vegetated channel [65], and attempts were made to emphasize the influence of bedforms. Thus, this section provides an analysis of the different proposed models.

It is important to mention that the methodologies found in the literature for the experimen-tal estimation of bedload transport in vegetated channels vary widely. The differences concern the way the tests were carried out (e.g., sediment supply rate in the initial section, duration of the tests) and the methodologies used. In some cases, sediments were not supplied at the upstream end [4], so that the bedload transport was only due to bed erosion; in others, sedi-ments were supplied continuously by, for example, a conveyor belt [2], or were recirculated [56, 65]. The tests durations are also very different. In the tests of Kothyari et al. [4] the test duration was short and varied from 1 min for supercritical flow to 4 min for subcritical flow; the tests of Cavedon [66], based on reaching a condition of uniform flow, had a minimum duration of 5 h and a maximum of 5–6 days. With regard to the estimation of the bedload transport, some researchers performed a direct measurement by collecting sediment in net bags [56], while others estimated it from image sequences recorded with a high-speed video camera mounted above the flume [67]. Also, the range of variation of the velocity used in the

literature experimental tests was very different. These result in very heterogeneous data, which partially explains the errors in interpreting them with the proposed formulas.

3.1 Sediment transport formulas based on bed shear stress

The bedload transport in a stream, Q_s, depends on the bed shear stress. For unvegetated streams, the critical shear stress is defined in terms of the flow condition and sediment characteristics by the Shields criterion. The bed shear stress is calculated from a relationship derived from the balance of the downslope weight component of the flow and the shear force at the bed.

For computing sediment transport through a vegetated stream, a partitioning of the flow resistance into a bed shear stress and a vegetation drag force is necessary. The bed shear stress, responsible for sediment transport, is usually calculated as the difference between the total and the vegetation drags. More correctly, the bedform resistances should also be taken into account [68, 69]. Vegetation as well reduces bedload transport by decreasing the bed shear stress [70].

Jordanova and James [2] carried out two series of experiments using one sediment size, a stem diameter $D = 5$ mm, and a stem spacing in longitudinal and transverse direction of 25 mm. The experiments of Series A were performed under a constant discharge per unit width $q = 6.5$ l/s/m, with four sediment supply rates per unit width, q_s, ($5.0 \leq q_s \leq 18.4$ g/s/m); the experiments of Series B were carried out under a constant sediment supply rate per unit width $q_s = 8.5$ g/s/m, with five discharges per unit width ($3.4 \leq q \leq 18.5$ l/s/m). The shear stress exerted on the bed, τ, for flow through emergent stems was calculated by subtracting the total stem drag from the total force applied by the flow in the flow direction. In carrying this out, the single stem drag coefficient was adjusted to account for the influence of multiple stems on the local velocity, on the basis of the indications of Li and Shen [71] and using their equation to determine the local velocity.

On the basis of the results belonging to Series A, Jordanova and James [2] proposed the following equation for the bedload sediment transport:

$$q_s = 0.017 (\tau - \tau_c)^{1.05}, \tag{13}$$

where τ_c is the critical value of bed shear stress. This equation was obtained with $R^2 = 0.99$, an average absolute error of 4.54%, a maximum error of -6.5%, and a standard deviation of 2.16%. The same equation was applied to predict the sediment input values for each experiment of Series B. Using the critical bed shear stress determined from the Shields diagram (0.23 N/m^2), it gave a prediction with an error of 16.9%.

Kothyari et al. [4], starting from a literature relationship for the bedload transport rate in open-channel flows without vegetation, proposed the following relationship:

$$\frac{q_s}{\sqrt{\Delta g d^3}} = 4.7 \tau_*^{3/2} \left(1 - \frac{\tau_{*c}}{\tau_*} \right) \frac{1}{(0.875 - S)}, \tag{14}$$

where $\tau_* = u_*^2 / (\Delta g d)$ is the non-dimensional shear stress, τ_{*c} is the non-dimensional critical shear stress (Shields parameter), u_* is the shear velocity, and S is the slope of the energy line. In the hypothesis that S is much smaller than 0.875, Eq. (14) can be simplified as follows:

$$\frac{q_s}{\sqrt{\Delta g d^3}} = 5.37\tau_*^{3/2}\left(1 - \frac{\tau_{*c}}{\tau_*}\right), \tag{15}$$

This equation was used to interpret the experimental data obtained from the tests performed by Kothyari et al. [4] and the data from Jordanova and James [2] and Baptist [72]. With reference to the experimental data of Kothyari et al. [4], it should be noted that no sediment was supplied during the tests from the upstream flume end, therefore this represents the natural erosion process. The adaptation of Eq. (15) to the experimental data returned errors greater than 200% in 30% of the data. These errors are also present in channels without vegetation and, according to Kothyari et al. [4], are to be attributed to measurement errors. It should be noted that the experimental data were related to both emergent rigid vegetation and submerged flexible vegetation.

Duan and Al-Asadi [68] conducted 18 laboratory experiments in an open-channel flume to study the impact of vegetation on bedform resistance and bedload transport. They considered the total flow resistance as constituted by the resistance of the bed, the walls and the vegetation. Bed resistance was further considered to be constituted by grains and bedform resistances. The latter was derived from semi-empirical relationships of bedform characteristics (height and length) in non-vegetated channels. They resulted in a relationship in which the following dimensionless groups were present: Froude number, ratio between the flow depth and the sediment diameter, vegetation density, and mobility parameter (defined as: (grain resistance)/[(critical resistance)-1]). The bedload transport rate was considered as the product of the bedload particle velocity and the thickness of the bedload layer. To obtain the bedload particle velocity the authors applied the exponential of the vegetation concentration to scale the bedload velocity for non-vegetated channels. In the same way, they calculated the thickness of the bedload layer using the vegetation density and two coefficients. For the estimation of these latter, the authors considered, in addition to their own experimental data, the data from Jordanova e James [2] and Kothiary et al. [4], using an optimization technique (the downhill simplex method—DSM) to determine the minimum or maximum value of an objective function in a multidirectional space. Duan and Al-Asadi [68] maximized the Nash–Sutcliffe Efficiency (NSE) coefficient and calculated the coefficients of determination between the predicted values from the relationships and the estimated ones. In the case of the bedform resistance law, the low value of the NSE required a new definition of the exponents of the dimensionless groups and the multiplicative constant. Both the bedform resistance equation (Eq. (30) in [68]) and that of the sediment transport (Eq. (31) in [68]) obtained by the authors seem to provide good results. Based on the equations, the bedform resistance increases with vegetation density, while bedload transport rate decreases.

Lu et al. [73] developed a theoretical method to estimate the bed shear stress based on the phenomenological theory of turbulence. In the case of unvegetated flows, the bed shear stress associated with sediment motion is closely related to the combined effects of bulk-flow-scale and grain-size-scale eddies and, considering the bed resistance as the momentum exchange of the flow due to the eddies near the bed, it is a function of fluid density, mean velocity of flow, grain diameter and hydraulic radius [73, 74]. In the presence of vegetation in the near-bed zone there are the vegetation-induced eddies and the grain-induced eddies. The vegetation-induced eddies, in the case of sparse vegetation, are governed by the vegetation stem diameter, instead, in the case of dense vegetation, they are constrained by the local stem spacing. The particle mobility is governed by the near-bed eddies of size equal to the grain diameter. For the determination of the characteristic

velocity of large eddies the authors referred to the dissipation rate of the TKE evaluated by the power associated with large eddies per unit mass. The characteristic velocity depends on the bulk-averaged velocity and the drag coefficient of vegetation. The authors expressed the bed shear stress as a function of fluid density, bulk-averaged velocity, drag coefficient of vegetation, grain diameter, vegetation diameter and vegetation density. Lu et al. [73] applied the bedload transport formula proposed by Cheng (Eq. (7) in [75]), initially derived for unvegetated flows, to 158 sets of literature data [2, 56, 65, 67, 76, 77] for vegetated flow conditions that cover all regimes, from extremely weak to high. The calculated values represent well the experimental data when the sediment diameter is in the inertial subrange [73]. The model was also applied to bedload transport data in the presence of vegetation patches [76] by considering average values within the patch for the velocity and drag coefficient. The results are satisfactory even though the range of variation of the dimensionless shear stress values is limited.

3.2 Sediment transport formulas based on the TKE

Yager and Schmeeckle [67] conducted a set of 12 flume experiments, in which uniform sand (having a median diameter of 0.5 mm) was transported through staggered arrays of 1.3 cm in diameter emergent cylinders, which were used to simulate rigid vegetation. They analyzed the flow patterns around vegetation and the bedload transport. Yager and Schmeeckle [67] measured the spatial and temporal variations in the downstream and vertical velocities using the Particle Imaging Velocimetry (PIV) and the spatial and temporal variations in sand transport at 250 frames/s using a high-speed camera mounted above the flume. Local sediment transport rates were calculated using a Fortran code, that determined the difference in pixels (due to sand movement) though cross-correlation analyses between two successive video-frames. Yager and Schmeeckle [67] observed that vegetation significantly increases the spatial variability in bedload flux; the highest fluxes occurred immediately adjacent to and downstream of vegetation, with relatively low fluxes in the intervening area between vegetation stems. For the same flow velocity, an increase in vegetation density caused higher mean and standard deviation in bedload fluxes. Conversely, for the same τ, vegetation density did not affect the mean bedload fluxes. Yager and Schmeeckle [67] highlighted that sweeps and bursts were more important upstream of vegetation, and inward and outward interactions were greater downstream, both along the water depth and particularly near the bed. The inward and outward interactions downstream of the vegetation may be due to the highly local vertical flow and oscillating von Kármán vortices produced by the vegetation. Outward interactions may be responsible for high sediment fluxes downstream of vegetation. High sediment fluxes immediately upstream and adjacent to vegetation may be caused by horseshoe vortices, which can locally increase the turbulence. Low bedload fluxes among vegetation stems were localized where the intensity of turbulence was reduced, and sediment deposition here may be caused by von Kármán vortices. Yager and Schmeeckle [67] highlighted that bursts and sweeps dominate in the case of submerged vegetation, whereas inward and outward interactions increase toward the bed in the case of emergent vegetation.

Yang and Nepf [56] carried out experimental tests in a channel, with a width equal to 1 m and a length equal to 10 m, both in the absence and in the presence of emergent vegetation. The vegetation was simulated by means of aluminum dowels with diameter $D = 6.3$ mm arranged in a staggered manner in a variable number from 0 to 810 m^{-2}. The frontal area of the vegetation per unit volume was $a = nD = 0$ to 5.1 m^{-1}, where n is the

number of cylinders, and the solid volume fraction of the vegetation was $\phi = (\pi/4)nD^2 = 0$ to 0.025. The dowels were placed across the entire width of the channel, and for a length of 3 m for lower densities and 2 m for higher densities. The bottom in the section of interest consisted of sand with a diameter between 0.42 and 0.60 mm, with median dimension $d = 0.5$ mm. Yang and Nepf [56] calculated the instantaneous bedload transport rate, defined as the mass of sand passing through the channel cross-section per time per unit width. The measurements were conducted several times. The average and standard error of all the measured bedload transport rates were used to represent the equilibrium bedload transport rate, q_s, and its uncertainty, σ_{qs}. Yang and Nepf [56] then measured the velocity profile up to 4 cm above the bed using a Nortek Vectrino profiler, under equilibrium conditions, and on a number of points ranging from 8 to 34. Measurements at 2 cm relative to the time-averaged bed elevation were used to represent the near-bed condition. From these, the authors first calculated the local near-bed TKE and the local near-bed Reynolds stress, $-\rho\left(\overline{u'w'}\right)$, for each point as representative of the near-bed values and, therefore, the respective spatial mean values and standard error. In the case of a vegetated channel, the TKE at 2 cm height is representative of the maximum value near the bed, whereas in the case of a non-vegetated channel it is underestimated by up to 30%. The authors pointed out that, for the same velocity, experimental tests with a greater fraction of the solid volume of the vegetation show a higher bedload transport rate. The model proposed by Einstein [78] and Brown [79], considering as dimensionless shear stress the one calculated from the measured value, fitted the experimental data of the dimensionless sediment transport rate well in the absence of vegetation, but, in the case of the vegetated channel, the experimental values of the sediment transport were significantly higher than those predicted by the model. Similar results were obtained by the authors considering the bed shear stress actually exerted on the bottom of the channel and estimated using the procedure suggested by Yang et al. [13].

Yang and Nepf [56], converted the Einstein-Brown model based on the shear stress to a model based on the TKE. In the case of a non-vegetated channel without bedforms, $k_t = \tau/(0.19\rho)$ and, considering its dimensionless form $\tau_* = 0.19k_{t*}$ ($k_{t*} = \frac{k_t}{\left(\frac{\rho_s}{\rho}-1\right)gd}$) in the equation of Einstein-Brown, the following expression was derived:

$$q_{s*} = \begin{cases} 2.15e^{-2.06/k_{t*}}, & k_{t*} < 0.95 \\ 0.27k_{t*}^3, & 0.95 < k_{t*} < 2.74 \end{cases} \tag{16}$$

This model, applied to the experimental data obtained by the authors and the data of Yager and Schmeeckle [67], gave much better results from a graphical viewpoint than the τ-based Einstein-Brown model. This is also confirmed by the root-mean-square deviation. Finally, the authors analyzed how the bedload transport varies with the vegetation solid volume fraction, considering that it also affects the flow velocity. Both the τ-based and the k_t-based model predicted a decrease in q_{s*} by increasing the solid volume fraction of the vegetation, but the q_{s*} predicted by the τ-based model was consistently smaller than that determined with the k_t-based model. However, this latter was more in line with the experimental results.

In a subsequent work, Yang and Nepf [64] applied the aforementioned model to a larger number of experimental bedload transport data available in the literature [2, 4, 67], which were obtained using different methodologies. They employed statistics of individual grain movement to understand the connection between turbulence and bedload transport, and analyzed the impact of vegetation on the bedform characteristics and migration rate. In the

various experimental tests, the vegetation was represented by rigid cylinders, arranged in a staggered manner. The drag coefficient was calculated using the following relationship [80]:

$$C_D = \zeta^2 \left[1 + 10 \left(\frac{\zeta VD}{\nu} \right)^{-2/3} \right], \tag{17}$$

where ζ represents the ratio of the average velocity between adjacent cylinders to the pore velocity and is given by $\zeta = (1 - \phi)/\left(1 - \sqrt{2\phi/\pi}\right)$. Equation (4) with the bed turbulence expressed as $\tau/(0.19\rho)$ and with $\delta_{k_t} = 0.4$ well interprets the values of the TKE found experimentally by the authors and those of Yager and Schmeeckle [67]. The TKE generated by the bed is greater than that generated by the vegetation when the vegetation volume fraction is less than 0.01; for greater values, the opposite occurred. From the estimated TKE, the authors calculated the bedload transport by also referring to the data of Yager and Schmeeckle [67], Kothyari et al. [4] and Jordanova and James [2], and carried out the estimation with the bed stress model. The results already obtained by Yang and Nepf [56] confirmed that the k_t-based model predicted the bedload transport in vegetated channels better than the τ-based model. In particular, the former predicted the bedload sediment transport values within one order of accuracy, whilst the latter underestimated it by several orders of magnitude. Thus, it was demonstrated that the bedload transport can be predicted from velocity and vegetation volume fraction. Since the channel-scale bedload transport rate can also be calculated as $q_s = V_p \xi$, where V_p is the average velocity of the grain in motion and ξ is the volume of moving grains per unit bed area, Yang and Nepf [64] used the statistics of individual grain motion to examine the influence of turbulence on bedload transport rate. For bare channels, V_p is proportional to V, whereas for vegetated channels V_p/V roughly increases with the solid volume fraction.

The greater turbulence levels likely lifted individual particles farther from the bed and the distance the particle is lifted up from the bed should also scaled with k_t. The lifted particle is accelerated by the streamwise velocity to which it is exposed, such that the particle's streamwise velocity, V_p, should depend on both V and the distance the particle is lifted up, which is proportional to the TKE. On the basis of the experimental results, Yang and Nepf [64] showed that V_p scales with $V + 10\sqrt{k_t}$ and ξ is also a function of both V and k_t, but the influence exerted by k_t is greater. The bedload transport rate is a function of both V_p and ξ; since both of these quantities are essentially a function of the TKE, it is evident that the bedload transport rate is a function of the latter, further confirming the authors' hypothesis. They noted, however, that in the experimental tests the range of velocity values was limited and, therefore, a dependency on it cannot be excluded.

Yang and Nepf [64] also analyzed in the same experiments the bedforms and the migration period. They were detected using a Vectrino profiler and a Keyence laser sensor. The bedforms consisted of ripples, with heights of less than 2 cm that decreased as the density increased, anticipating the formation of an upper-regime plane bed. For lower densities, the ripple wavelength depended on the distance between the vegetation and the ripple migration velocity increased with flow velocity as well as density, again confirming the influence of turbulence on bedload transport. The fact that at high vegetation densities the bedforms were no longer present does not allow the bedload transport to be estimated from the ripple migration velocity under these circumstances.

Wu et al. [77] carried out experimental tests in a 12 m-long, 0.6 m-wide and 0.6 m-deep slope-adjustable flume, in which a 10 cm-thick layer of sand was created over a length of

8 m. The median diameter of the uniform sediments was $d = 0.931$ mm. The vegetation was simulated using circular cylindrical elements of fiberglass in a staggered array. The cylinders occupied a length of 5 m and were held upright by two plastic plates. Two different diameters were used, namely 7.8 mm and 10 mm. The flow depth was 30 cm. Tests were conducted until the equilibrium condition was reached and the bedload transport rates was measured. Wu et al. [77] conducted 56 experimental tests in the presence of vegetation and 4 tests without vegetation. Wu et al. [77] analyzed the spatial variability of the sediment exchange using qualitative tests. To this end, before starting the test, they colored the surface sediment layer in black at the end of the vegetated section having a length of 1 m to analyze the areas of erosion and deposition. Moreover, they colored two lateral strips, 1 m long but approximately 3 cm thick, located upstream, to analyze the lateral dispersion of sediment transport. When the sediments were eroded, the underlying sediments appeared light brown in color; instead, the areas that remained black were the areas not affected by sediment exchange. Once the stems were removed, photos were taken to make observations on the spatial variability of sediment transport. Depending on the flow rate, it was possible to observe sediment transport near individual stems or a global exchange of sediment over the entire bed. The authors classified the bedload transport into three different regimes:

- Regime 1, local sediment motions: the sediment particles move in very limited areas around the cylinders and in practice there was no bedload transport;
- Regime 2, incomplete global sediment transport: it occurs for high flow intensities; there is movement of particles in the longitudinal direction, i.e., the particles are transported from the scour hole around one cylinder to the next cylinder; however, there is no movement in the transverse direction;
- Regime 3, complete global sediment transport: it occurs at an even higher flow intensity, and sediment transport affects all areas of the river bed with lateral dispersion of sediment; sediment is transported from the area around a cylinder to the cylinders downstream in a diagonal direction. This regime is facilitated by a high density of vegetation.

Wu et al. [77] proposed a model capable of evaluating the bedload transport in the case of Regime 2 (i.e. weak transport) and for moderate transport in Regime 3. However, the model can also be used in Regime 3 when the lateral dispersion is negligible compared to the longitudinal component of the transport. Starting from the data collected by Yager and Schmeeckle [67], Wu et al. [77] reconstructed the scalar and vector fields of the bedload fluxes, which showed that the bedload transport rate immediately downstream of the cylinders, and immediately laterally, was very intense and equal to about 10 times the lateral one. The authors claimed that it is very unlikely that a generic particle could pass between the cylinders without being deposited in the hole around the cylinders and then dragged out. It follows that, in order to determine the bedload transport, it is first necessary to evaluate the transport in the scour holes located at a cross-section and then to add up the different contributions appropriately. The analysis of the vector field of the bedload fluxes showed that it is possible to identify a section downstream of a cylinder, where the vectors are characterized, in practice, only by longitudinal components of the bedload fluxes. Furthermore, this section can be divided into two areas: one, downstream of the cylinder, characterized, as already mentioned, by a strong intensity, and the other, moving towards the other row of cylinders, by a weak intensity. Note that in the two areas the bedload sediment transport is equal. The authors also analyzed the bed morphology that is formed as a result of the presence of vegetation. In particular, for the weakest sediment transport, in addition

to the scour holes around the cylinders, dunes were formed connecting the scour holes with the downstream cylinder. The shape of these dunes gave indications on the trajectories of sediment transport, which occurred only along the longitudinal direction and is characteristic of Regime 2. For the most intense sediment transport, the bedforms covered the entire bed and the holes around the cylinders were connected by the saddle-shaped bedforms to the cylindrical elements on the other row according to the diagonals. As mentioned, in Regime 2 the bedload transport occurs along the lines joining the cylinders in the flow direction, so that the bedload transport in a cross-section is given by the sum of the transport along the different lines and, if all the stems have the same size, it can be determined from the sediment motion around a single stem. If the latter is correctly evaluated and the lateral dispersion is negligible, the proposed model can also be used in Regime 3. With reference to a row of cylinders, Wu et al. [77] defined the dimensionless bedload transport rate per unit width, $q^*_{s,W}$, as follows:

$$q^*_{s,W} = \frac{q_B}{\sqrt{g\Delta d^3}} \frac{L_{y,s}}{2D} \tag{18}$$

The representative parameter of the spatially average flow condition, Θ_V, was defined by:

$$\Theta_V = \frac{V^2}{g\Delta d}. \tag{19}$$

Estimating erosion around a single cylinder is an extremely complex phenomenon [67, 81–84], and Wu et al. [77], simplifying, claimed that it depends essentially on the TKE on the bed. The latter is given by the sum of the kinetic energy of the mean flow upstream of the cylinder (which is transformed into the TKE) and the TKE also upstream of the cylinder. Defining K_V as the ratio of the spatially averaged TKE, k_t, to the bulk flow kinetic energy, $V^2/2$, i.e., $K_V = 2k_t/V_t^2$, the TKE of the flow near the bottom in the area close to the cylinders, subject to the intense movement of the particles, is approximately equal to $V^2(1 + K_V)/2$. One can refer to Wu et al. [77] for the methodology adopted to estimate K_V.

For uniform cylinder and grain sizes, the flow intensity around the stems in the aforementioned area is given by:

$$\Theta_{V\Omega} = \Theta_V \left(1 + K_V\right)^m, \tag{20}$$

where m is a calibration exponent ($m > 1$). To consider the influence of the grain and cylinder sizes, the authors modified the hydrodynamic parameter as:

$$\Theta^*_{V\Omega} = \left(C_\Omega \Theta_{V\Omega}\right)^{exp(C_d d/D)}, \tag{21}$$

where C_Ω and C_d are constants to be determined on the basis of experimental data. Based on their own experimental data and those taken from the literature [56, 65, 67], they estimated the values of m, C_Ω and C_d obtaining that $m = 4$, $C_\Omega = 0.22$, and $C_d = 1.15$. From the experimental data, the link between $\Theta^*_{V\Omega}$ and $q^*_{s,W}$ was represented by the following power function, with a good coefficient of determination ($R^2 = 0.956$):

$$q^*_{s,W} = \frac{\left(\Theta^*_{V\Omega}\right)^{1.63}}{240}. \tag{22}$$

The data of Wu et al. [77] were well interpreted, unlike those of the other authors. The model of Wu et al. [77] is applicable in the case of weak or moderate bedload transport rate and in the case of sparse distribution characterized by $2D / \left(L_{x,s}^2 + L_{y,s}^2 \right)^{1/2} < 0.56$.

3.3 Modified classical sediment transport formulas

Vargas-Luna et al. [85] verified the applicability of the formulas of Engelund and Hansen [86] and Van Rijn [87], derived for a bare bed, to the data of Jordanova and James [2] and Kothyari et al. [4], calculating the average velocity and bed shear stress with the models of Barfield et al. [88], Stone and Shen [89], and Baptist [72]. In some cases, the methods of Stone and Shen [89] and Baptist [72] provided bed shear stresses lower than the critical value, so that in these cases the sediment transport with the formula of van Rijn [87] was null. The results showed that for high sediment transport rate the two formulas provided similar results, whereas for low sediment transport rate the formulas of Engelund and Hansen [86] provided better results, even though they showed considerable deviations.

Armanini et al. [90], starting from the Einstein [78] theory, proposed a theoretical model for the estimation of bedload sediment transport in riverbeds called ballistic model. The main novelty of the model is the definition of the probability that a particle reaches the section where the sediment transport rate is calculated. It is assumed to be equal to the product of two independent probabilities: the probability associated with the lifting of the grains and that associated with the particles being able to travel the distance from the point at which they are lifted to the section of interest. The authors adopted the Gamma distribution for both and obtained the sediment transport rate by integrating the distribution of the ranges of the particle jumps multiplied by the average particle velocity. The particle velocity was assumed to depend on the shear velocity and on the flow intensity parameter, whereas the average particle range was a hyperbolic function of the flow intensity. The authors also considered the probability of each particle colliding with other particles.

Armanini and Cavedon [65] applied the above model to directly measure experimental data in a mobile-bed channel with emergent vegetation. The authors expressed the flow intensity parameter as a function of the grain shear stress in a first case, and, in a second case, as a function of the total resistance. In the first case, they obtained an underestimation of the experimental values, whilst in the second case an overestimation. Based on the observation that the experimental values for the different densities were substantially similar to the model predictions (valid in the absence of vegetation), the authors redefined the flow intensity parameter using the momentum analysis, with two parameters to be determined experimentally. A further effect of the presence of vegetation is the reduction of the active exchange surface between stream and bed, and, on the other hand, the fact that the area around the vegetation is subject to excavation and once excavated contributes less to sediment transport. To consider this, Armanini and Cavedon [65] modified the definition of dimensionless sediment transport in vegetated beds by using a parameter to be determined experimentally. Finally, to consider the influence of viscosity when transporting plastic material, they introduced an effective diameter in the definition of the flow intensity parameter. The model applied to their experimental data showed good results. Since the model consisted of a redefinition of the dimensionless sediment transport rate and flow intensity parameter, it could also be applied to other formulas of bedload transport based on the two aforementioned dimensionless groups. Armanini and Cavedon [65] applied it, with reference to their own experimental data, using the formulas of Meyer-Peter and Müller [91],

Parker [92], and van Rijn [87] and obtained results that presented errors comparable to those usually accepted for this type of problem.

Bonilla-Porras et al. [93] extended the model of Armanini and Cavedon [65] to submerged vegetation. The authors estimated the model parameters on the basis of their own experimental tests and validated the model by referring to literature data. It should be noted that field data from flexible vegetation were also used in the validation. Comparison with other models proposed in the past and based on the statistical measures, i.e., mean absolute error, mean relative error, root mean square and determination coefficient, showed the improved ability of the model to interpret the data.

3.4 Sediment transport for vegetated banks

Specht and Koll [94] analyzed the influence of bank vegetation on the bedload transport in a channel without vegetation. The flow velocity in the vegetated area was smaller than the one in the channel. This determined a secondary flow that was directed towards the center of the channel close to the bed, while it was directed towards the banks near the surface. This secondary flow caused a scour hole close to the banks. The area of the bed influenced by vegetation decreases as the width of the channel increases. The authors pointed out that for narrow channels and densely vegetated banks, the bed-load transport calculated with the usual literature formulas is underestimated. As a result, they provided relationships that allow the evaluation of a coefficient that when multiplied by the estimated bedload transport in the channel in the absence of vegetation on the banks returns the bedload transport in the presence of vegetation. The proposed model also considers the presence of vegetation on a single bank. The influence of vegetation on bedload transport vanished when the ratio of the width of the non-vegetated part of the water surface to the height of the vegetated part on the banks is greater than 6.

4 Effect of vegetation on bed morphology

Penna et al. [95] conducted flume experiments to investigate the effect of streambed instability in channels with randomly-distributed vegetation, varying vegetation density (34 and 68 cylinders of $D = 2$ cm inserted into a panel 1.96 m long and 0.485 m wide, with a density of 1.12% and 2.25%, respectively) and flow conditions ($Q = 11.85$ l/s and 19.85 l/s), in the absence of upstream sediment supply, so that the sediment transport was originated solely from the erosive action of the flow on the bed or near the stems. The topography of the bed surface was acquired with photogrammetric techniques at the beginning of each experiment, with the sediment placed at the bottom with the same slope as the channel, and at the end of each experiment, when the bedload transport rate was 1% of that measured at the beginning. A bilinear detrending algorithm was applied to the structured grids to remove the respective surface bed slopes, which could obscure the bed surface properties, while also the mean bed elevation was removed from the bed elevation data. Finally, the surfaces at the meso- and micro-scale were extracted from the measured grids. The introduction of vegetation caused a reduction of the sediment transport: it decreased as the vegetation density increased, with much more efficiency in the case of high flow intensity. Therefore, the presence of vegetation contributes in promoting the stability of the streambed. In the case of a non-vegetated channel and owing to the higher discharge,

the formation of multiple bars was observed. In runs with low vegetation density, scour holes were observed in correspondence with the stems, while dunes displayed an elongated shape along the streamwise direction, implying that the trajectory of sediment transport was predominantly in the longitudinal direction. By increasing the vegetation density, the bed structures became shorter than before and they resulted to be laterally expanded, owing to the obstruction created by the stems, that originated both longitudinal and lateral sediment transport. The analysis of longitudinal and transverse profiles, given the density of vegetation and the diameter of the cylinders and sediments, showed a good overlap, i.e., the bed morphology configuration does not depend on the flow rate; this latter affects only the magnitude of bed degradation.

5 Conclusions and future research

The present review summarizes recent research results and highlights on how emergent rigid vegetation affects incipient sediment motion and bedload transport. This is only one of the complex research aspects due to the presence of vegetation in rivers, estuaries, marshes, mangrove forests, seagrass meadows [54]. Indeed, the presence of vegetation is recognized to create a complicated system of feedbacks and linkages between channel flow, morphology, sediment deposition and erosion, density and spatial extent [96]. The paper concerns only one of the possible vegetation types and sediment transport, that is the emergent rigid vegetation and the bedload transport, showing as, notwithstanding the great progress made in recent years, further research is needed [85]. In this limited, but important context, focus should be made to evaluate both the flow field and the transport rates.

All formulas relating to the incipient sediment motion and the estimation of bedload transport rate in the presence of vegetation were obtained from experimental tests conducted by representing vegetation using cylindrical elements of different material and flexibility. Although in some cases the cylindrical elements are an accurate representation of some types of plants [54, 93, 97], in many cases they do not represent the different characteristics of real vegetation, which, in addition, differ among species both seasonally and over time. It would be advisable to conduct laboratory tests with natural vegetation and verify the validity of the various formulas proposed in the literature. Even better it would be to carry out extensive and detailed field measurement campaigns on velocity, turbulence and sediment transport with reference to different climatic conditions, vegetation species, hydraulic and environmental conditions, which would require improvement of measurement techniques and instrumentation. This would allow the accuracy of the various formulas proposed in the literature to be verified in real cases.

Many of the experimental studies analyzed in Sects. 2 and 3 were conducted with a flat bed and constant slope. It would be appropriate carrying out measurements of bedload transport rate in the presence of bedforms, extending the work of Wu et al. [77], according to their classification, to the case of complete global sediment transport. Nevertheless, one should note that upscaling the laboratory results to real conditions needs choosing the best dimensionless parameters, and this point is not easy [12].

The various tests illustrated referred to vegetation arranged in an orderly manner (linear or staggered) in fully covered channels, i.e., with the vegetation occupying a long stretch of the watercourse. Most formulas consider the drag coefficient, that, even if used by generations of engineers, still present many uncertainties, and more in the presence of bedload transport. The various formulas should be extended, possibly by means of corrective

coefficients, to the case of random distribution. However, in real rivers the vegetation is often arranged in patches of limited size and frequently approximately circular. Several studies were conducted on sediment deposition around patches of vegetation [98–101]. More attention should be paid to erosion and sediment transport in the presence of vegetation patches, also analyzing the influence on morphology and plant growth; in this case appropriate space and time scales should be considered. Moreover, according to some researchers, shear stress is not the best physical variable to account for in case of incipient sediment motion through vegetation [12].

It is appropriate to study the interaction between water flow, vegetation and sediments with combined methods based on laboratory observation, in the field and through numerical simulations. This would allow a mutual and independent validation of the different methodologies. Turbulent coherent structures and their modification with bedload transport should be investigated, in order to possibly find their influence into numerical simulations.

In conclusion, as usual, in many research fields, the more advances in the knowledge of phenomena are achieved, the more new aspects appear to need further investigation and effort.

Declarations

References

1. Bennett SJ, Simon A (2004) Riparian vegetation and fluvial geomorphology. American Geophysical Union, Washington, DC, USA
2. Jordanova AA, James C (2003) Experimental study of bed load transport through emergent vegetation. J Hydraul Eng 129(6):474–478
3. EU, Directive 2007/60/EC of the European Parliament and of the Council of 23 October 2007 on the Assessment and Management of Flood Risks. 2007. Available online: https://eur-lex.europa.eu/legal-content/EN/TXT/?uri=celex:32007L0060 (Accessed on 20 Apr 2022)
4. Kothyari U, Hashimoto H, Hayashi K (2009) Effect of tall vegetation on sediment transport by channel flows. J Hydraul Res 47(6):700–710
5. Curran JC, Hession WC (2013) Vegetative impacts on hydraulics and sediment processes across the fluvial system. J Hydrol 505:364–376

6. Christiansen T, Azlak M, Ivits-Wasser E (2020) Floodplains: a natural system to preserve and restore; EEA Report 24/2019. European Environment Agency: Luxembourg

7. Verheij S, Fokkens B, Buijse AD (2021) A pan-European survey to strengthen and improve policies and strategic planning regarding river continuity restoration. STOWA, Utrecht

8. Anderson BG, Rutherfurd ID, Western AW (2006) An analysis of the influence of riparian vegetation on the propagation of flood waves. Environ Model Softw 21(9):1290–1296

9. Rutherfurd ID, Anderson B, Ladson A (2007) Managing the effects of riparian vegetation on flooding. In: Lovett S, Price P (eds) Principles for riparian lands management, Land and Water, Canberra (Australia), pp 63–84

10. Shields DF Jr, Coulton KG, Nepf H (2017) Representation of vegetation in two-dimensional hydrodynamic models. J Hydraul Eng 143(8):02517002

11. D'Ippolito A, Calomino F, Alfonsi G, Lauria A (2021) Flow resistance in open channel due to vegetation at reach scale: a review. Water 13(2):116

12. Huai W, Li S, Katul GG, Liu M, Yang Z (2021) Flow dynamics and sediment transport in vegetated rivers: a review. J Hydrodyn 33:400–420

13. Yang JQ, Kerger F, Nepf HM (2015) Estimation of the bed shear stress in vegetated and bare channels with smooth bed. Water Resour Res 51(5):3647–3663

14. Liu D, Valyrakis M, Williams R (2017) Flow hydrodynamics across open channel flows with riparian zones: implications for riverbank stability. Water 9(9):720

15. Afzalimehr H, Dey S (2009) Influence of bank vegetation and gravel bed on velocity and Reynolds stress distributions. Int J Sediment Res 24:236–246

16. Ben Meftah M, Mossa M (2013) Prediction of channel flow characteristics through square arrays of emergent cylinders. Phys Fluids 25(4):045102

17. Ben Meftah M, Mossa M (2016) A modified log-law of flow velocity distribution in partly obstructed open channels. Environ Fluid Mech 16(2):453–479

18. Caroppi G, Gualtieri P, Fontana N, Giugni M (2018) Vegetated channel flows: Turbulence anisotropy at flow–rigid canopy interface. Geosciences 8(7):259

19. Maji S, Hanmaiahgari PR, Balachandar R, Pu JH, Ricardo AM, Ferreira RM (2020) A review on hydrodynamics of free surface flows in emergent vegetated channels. Water 12:1218

20. Penna N, Coscarella F, D'Ippolito A, Gaudio R (2020) Anisotropy in the free stream region of turbulent flows through emergent rigid vegetation on rough beds. Water 12(9):2464

21. Penna N, Coscarella F, D'Ippolito A, Gaudio R (2020) Bed roughness effects on the turbulence characteristics of flows through emergent rigid vegetation. Water 12(9):2401

22. D'Ippolito A, Calomino F, Coscarella F, Gaudio R, Penna N (2022) Quadrant analysis of turbulence in vegetated channels. In: Frega G, Macchione F (eds) Technologies for integrated river basin management, Proceedings of Italian conference on integrated river basin management (ICIRBM), vol 43. EdiBios, Cosenza (Italy), pp 83–90

23. Sukhodolova T, Sukhodolov A (2012) Vegetated mixing layer around a finite-size patch of submerged plants: 1. Theory and field experiment. Water Resour Res 48(10):W10533

24. Sukhodolova AN, Sukhodolov TA (2012) Vegetated mixing layer around a finite-size patch of submerged plants: 2. Turbulence and coherent structures. Water Resour Res 48(12):W12506

25. Siniscalchi F, Nikora VI, Aberle J (2012) Plant patch hydrodynamics in streams: mean flow, turbulence, and drag forces. Water Resour Res 48:W01513

26. Yilmazer D, Ozan AY, Cihan K (2018) Flow characteristics in the wake region of a finite-length vegetation patch in a partly vegetated channel. Water 10(4):459

27. Yamasaki TN, de Lima PH, Silva DF, Cristiane GDA, Janzen JG, Johannes G, Nepf HM (2019) From patch to channel scale: the evolution of emergent vegetation in a channel. Adv Water Res 129:131–145

28. Cheng NS, Hui CL, Wang X, Tan SK (2019) Laboratory study of porosity effect on drag induced by circular vegetative patch. J Eng Mech 145(7):04019046

29. Liu C, Shan Y (2019) Analytical model for predicting the longitudinal profiles of velocities in a channel with a model vegetation patch. J Hydrol 576:561–574

30. Kitsikoudis V, Yagci O, Kirca VSO (2020) Experimental analysis of flow and turbulence in the wake of neighboring emergent vegetation patches with different densities. Environ Fluid Mech 20(6):1417–1439

31. Yan C, Shan Y, Sun W, Liu C, Liu X (2020) Modeling the longitudinal profiles of streamwise velocity in an open channel with a model patch of vegetation. Environ Fluid Mech 20(6):1441–1462

32. Mossa M, De Serio F (2016) Rethinking the process of detrainment: jets in obstructed natural flows. Sci Rep 6(1):1–11

33. Mossa M, Ben Meftah M, De Serio F, Nepf HM (2017) How vegetation in flows modifies the turbulent mixing and spreading of jets. Sci Rep 7(1):1–14
34. De Serio F, Ben Meftah M, Mossa M, Termini D (2018) Experimental investigation on dispersion mechanisms in rigid and flexible vegetated beds. Adv Water Resour 120:98–113
35. Termini D (2019) Turbulent mixing and dispersion mechanisms over flexible and dense vegetation. Acta Geophys 67(3):961–970
36. Mulahasan S, Stoesser T (2017) Flow resistance of in-line vegetation in open channel flow. Int J River Basin Manag 15(3):329–334
37. D'Ippolito A, Calomino F, Alfonsi G, Lauria A (2021) Drag coefficient of in-line emergent vegetation in open channel flow. Int J River Basin Manag 15(3):1–11
38. Errico A, Lama GFC, Francalanci S, Chirico GB, Solari L, Preti F (2019) Flow dynamics and turbulence patterns in a drainage channel colonized by common reed (Phragmites Australis) under different scenarios of vegetation management. Ecol Eng 133:39–52
39. Lama GFC, Errico A, Francalanci S, Solari L, Preti F, Chirico GB (2020) Evaluation of flow resistance models based on field experiments in a partly vegetated reclamation channel. Geosciences 10(2):47
40. Stoesser T, Kim SJ, Diplas P (2010) Turbulent flow through idealized emergent vegetation. J Hydraul Eng 136:1003–1017
41. Kim SJ, Stoesser T (2011) Closure modeling and direct simulation of vegetation drag in flow through emergent vegetation. Water Resour Res 47(10):W10511
42. Marjoribanks TI, Hardy RJ, Lane SN (2014) The hydraulic description of vegetated river channels: the weaknesses of existing formulations and emerging alternatives. WIREs Water 1:549–560
43. Forzieri G, Degetto M, Righetti M, Castelli F, Preti F (2011) Satellite multispectral data for improved floodplain roughness modelling. J Hydrol 407:41–57
44. Forzieri G, Castelli F, Preti F (2012) Advances in remote sensing of hydraulic roughness. Int J Remote Sens 33(2):630–654
45. Jalonen J, Järvelä J, Virtanen JP, Vaaja M, Kurkela M, Hyyppa H (2015) Determining characteristic vegetation areas by terrestrial laser scanning for floodplain flow modeling. Water 7:420–437
46. Huylenbroeck L, Laslier M, Dufour S, Georges B, Lejeune P, Michez A (2019) Using remote sensing to characterize riparian vegetation: a review of available tools and perspectives for managers. J Environ Manag 267:110652
47. Lama GFC, Crimaldi M, Pasquino V, Padulano R, Chirico GB (2021) Bulk drag predictions of riparian *Arundo donax* stands through UAV-acquired multispectral images. Water 13:1333
48. Flatley A, Rutherford I, Sims A (2022) Using structure-from-motion photogrammetry to improve roughness estimates for headwater dryland streams in the Pilbara, Western Australia. Remote Sens 14:454
49. da Silva AR, Demarchi L, Sikorska D, Sikorski P, Archiciński P, Jóźwiak J, Chormański J (2022) Multi-source remote sensing recognition of plant communities at the reach scale of the Vistula River, Poland. Ecol Indic 142:109160
50. Liu D, Diplas P, Fairbanks JD, Hodges CC (2008) An experimental study of flow through rigid vegetation. J Geophys Res 113(F4):F04015
51. Huai WX, Chen ZB, Han J, Zhang LX, Zeng YH (2009) Mathematical model for the flow with submerged and emerged rigid vegetation. J Hydrodyn 21(5):722–729
52. Huai WX, Zhang J, Katul GG, Cheng YG, Tang X, Wang WJ (2019) The structure of turbulent flow through submerged flexible vegetation. J Hydrodyn 31(2):274–292
53. Nepf H (2012) Hydrodynamics of vegetated channels. J Hydraul Res 50(3):262–279
54. Vargas-Luna A, Crosato A, Calvani G, Uijttewaal WSJ (2016) Representing plants as rigid cylinders in experiments and models. Adv Water Resour 93:205–222
55. Hongwu T, Wang H, Liang DF, Lv SQ, Yan L (2013) Incipient motion of sediment in the presence of emergent rigid vegetation. J Hydro-Environ Res 7(3):202–208
56. Yang JQ, Nepf HM (2018) A turbulence-based bed-load transport model for bare and vegetated channels. Geophys Res Lett 45(9):10428–10436
57. Yang J, Chung H, Nepf H (2016) The onset of sediment transport in vegetated channels predicted by turbulent kinetic energy. Geophys Res Lett 43(21):11261–11268
58. Cheng NS, Wei M, Lu Y (2020) Critical flow velocity for incipient sediment motion in open channel flow with rigid emergent vegetation. J Eng Mech 146(11):04020123
59. Wang X, Huai W, Cao Z (2022) An improved formula for incipient sediment motion in vegetated open channels flows. Int J Sediment Res 37(1):47–53
60. Zhang RJ, Xie JH, Wang MP, Huang JT (1998) River sediment dynamics, 2nd edn. China Water and Power Press, Beijing (China)

61. Wang H, Tang HW, Yuan S, Lü SQ, Zhao XY (2014) An experimental study of the incipient bed shear stress partition in mobile bed channels filled with emergent rigid vegetation. Sci China Technol Sci 57(6):1165–1174
62. Wang X, Li S, Yang Z, Huai W (2022) Incipient sediment motion in vegetated open-channels flows predicted by critical flow velocity. J Hydrodyn 34(1):63–68
63. Jeon HS, Obana M, Tsujimoto T (2014) Concept of bed roughness boundary layer and its application to bed load transport in flow with non-submerged vegetation. Water Resour Prot 6(10):881–887
64. Yang QJ, Nepf HM (2019) Impact of vegetation on bed load transport rate and bedform characteristics. Water Resour Res 55(7):6109–6124
65. Armanini A, Cavedon V (2019) Bed-load through emergent vegetation. Adv Water Resour 129:250–259
66. Cavedon V (2012) Effects of rigid stems on sediment transport. PhD Thesis, University of Trento (Italy)
67. Yager EM, Schmeeckle MW (2013) The influence of vegetation on turbulence and bed load transport. J Geophys Res 118(3):1585–1601
68. Duan JG, Al-Asadi K (2022) On bed form resistance and bed load transport in vegetated channels. Water 14:3794
69. Le Bouteiller C, Venditti J (2015) Sediment transport and shear stress partitioning in a vegetated flow. Water Resour Res 51:2901–2922
70. James CS, Jordanova AA, Nicolson CR (2002) Flume experiments and modelling of flow-sediment-vegetation interactions. IAHS Publication, Wallingford, pp 3–10
71. Li RM, Shen HW (1973) Effect of tall vegetations on flow and sediment. J Hydraul Div 99(5):793–814
72. Baptist MJ (2005) Modelling floodplain biogeomorphology. PhD Thesis, Delft University of Technology, The Netherlands
73. Lu Y, Cheng NS, Wei M (2021) Formulation of bed shear stress for computing bed-load transport rate in vegetated flows. Phys Fluids 33(11):115105
74. Gioia G, Bombardelli FA (2002) Scaling and similarity in rough channel flows. Phys Rev Lett 88:014501
75. Cheng NS (2002) Exponential formula for bedload transport. J Hydraul Eng 128(10):942–946
76. Shan Y, Zhao T, Liu C, Nepf H (2020) Turbulence and bed-load transport in channels with randomly distributed emergent patches of model vegetation. Geophys Res Lett 47:e2020GL087055
77. Wu H, Cheng NS, Chiew YM (2021) Bed-load transport in vegetated flows: phenomena, parametrization, and prediction. Water Resour Res 57(4):e2020WR028143
78. Einstein HA (1950) The bed-load function for sediment transportation in open channel flows (Technical Bulletin No 1026). US Department of Agriculture, Washington, DC
79. Brown CB (1950) Sediment transportation. Eng Hydraul 12:769–857
80. Etminan V, Lowe RJ, Ghisalberti M (2017) A new model for predicting the drag exerted by vegetation canopies. Water Resour Res 53:3179–3196
81. Neary VS, Constantinescu SG, Bennett SJ, Diplas P (2012) Effects of vegetation on turbulence, sediment transport, and stream morphology. J Hydraul Eng 138:765–776
82. Dey S, Raikar RV (2007) Characteristics of horseshoe vortex in developing scour holes at piers. J Hydraul Eng 133(4):399–413
83. Kirkil G, Constantinescu SG, Ettema R (2008) Coherent structures in the flow field around a circular cylinder with scour hole. J Hydraul Eng 134(5):572–587
84. Yagci O, Celik MF, Kitsikoudis V, Kirca O, Hodoglu C, Valyrakis M, Duran Z, Kaja S (2016) Scour patterns around isolated vegetation elements. Adv Water Resour 97:251–265
85. Vargas-Luna A, Crosato A, Uijttewaal W (2015) Effects of vegetation on flow and sediment transport: comparative analyses and validation of predicting models. Earth Surf Process Landforms 40(2):157–176
86. Engelund F, Hansen E (1967) A monograph on sediment transport in alluvial streams. Technical Report, Copenhagen, Danish Technical Press
87. van Rijn L (1984) Sediment transport, part I: bed load transport. J Hydraul Eng 110(10):1431–1456
88. Barfield BJ, Tollner EW, Hayes JC (1979) Filtration of sediment by simulated vegetation. I. Steady-state flow with homogenous sediment, transactions. Trans ASAE 22(3):540–545
89. Stone MC, Shen HT (2002) Hydraulic resistance of flow in channel with cylindrical roughness. J Hydraul Eng 128(5):500–506
90. Armanini A, Cavedon V, Righetti M (2015) A probabilistic/deterministic approach for the prediction of the sediment transport rate. Adv Water Resour 81(July):10–18

91. Meyer-Peter E, Müller R. (1948) Formulas for bed load transport. In: Proceedings of the 2nd IAHR congress, Stockholm (Sweden), pp 39–64
92. Parker G (1990) Surface-based bedload transport relation for gravel rivers. J Hydraul Res 28(4):417–436
93. Bonilla-Porras JA, Armanini A, Crosato A (2021) Extended Einstein's parameters to include vegetation in existing bedload predictors. Adv Water Resour 152:103928
94. Specht FJ, Koll K (2004) Adaptation of bed-load transport formulas for vegetated banks. In: Volume 2 "Model application for wetlands hydrology and hydraulics" of the Conference Wethydro - Center of Excellence in Wetland Hydrology, Bialistok (Poland)
95. Penna N, Coscarella F, D'Ippolito A, Gaudio R (2022) Effects of fluvial instability on the bed morphology in vegetated channels. Environ Fluid Mech 22(2):619–644
96. Hession WC, Curran JC (2013) The impact of vegetation on roughness in fluvial systems. In: Treatise on Geomorphology. vol. 12, Ecogeomorphology, Academic Press, San Diego (California, USA), pp 75–93
97. Wunder S, Lehmann B, Nestmann F (2011) Determination of the drag coefficient of emergent and just submerged vegetation. Int J River Basin Manag 9(3–4):231–236
98. de Lima PHS, Janzen JG, Nepf HM (2015) Flow patterns around two neighboring patches of emergent vegetation and possible implications for deposition and vegetation growth. Environ Fluid Mech 15:881–898
99. Liu C, Nepf H (2016) Sediment deposition within and around a finite patch of model vegetation over a range of channel velocity. Water Resour Res 52:600–612
100. Shi Y, Jiang B, Nepf HM (2016) Influence of particle size and density, and channel velocity on the deposition patterns around a circular patch of model emergent vegetation. Water Resour Res 52:1044–1055
101. Liu C, Hu Z, Lei J, Nepf HM (2018) Vortex structure and sediment deposition in the wake behind a finite patch of model submerged vegetation. J Hydraul Eng 144(2):04017065